

The Population of Deformed Bands in ^{48}Cr by emission of ^8Be from the $^{32}\text{S} + ^{24}\text{Mg}$ reaction

S. Thummerer¹, W. von Oertzen^{1,2}, B. Gebauer¹, S.M. Lenzi³,
A. Gadea⁴, D.R. Napoli⁴, C. Beck⁵, M. Rousseau⁵

¹ Hahn-Meitner-Institut Berlin, Glienicker Strasse 100, 14109 Berlin, Germany

² Freie Universität Berlin, Fachbereich Physik, Arnimallee 14, 14195 Berlin, Germany

³ INFN, Laboratori Nazionali di Legnaro, Via Romea 4, 35020 Legnaro(PD), Italy

⁴ Dipartimento di Fisica and INFN, Padova, Italy

⁵ Institut de Recherches Subatomiques, IN2P3-CNRS/Université Louis Pasteur, B.P. 28, F-67037 Stasbourg CEDEX 2, France

Abstract. Using particle - γ coincidences we have studied the population of final states after the emission of 2 α -particles and of ^8Be in nuclei formed in $^{32}\text{S}+^{24}\text{Mg}$ reactions at an energy of $E_L(^{32}\text{S}) = 130\text{ MeV}$. The data were obtained in a setup consisting of the GASP γ -ray detection array and the multidetector array ISIS. Particle identification is obtained from the ΔE and E signals of the ISIS silicon detector telescopes, the ^8Be being identified by the instantaneous “pile up” of the ΔE and E pulses. γ -ray decays of the ^{48}Cr nucleus are identified with coincidences set on 2 α -particles and on ^8Be . Some transitions of the side-band with $K^\pi = 4^-$ show stronger population for ^8Be emission relative to that of 2 α -particles (by a factor 1.5 – 1.8). This observation is interpreted as due to an enhanced emission of ^8Be into a more deformed nucleus. Calculations based on the extended Hauser-Feshbach compound decay formalism confirm this observation quantitatively.

PACS numbers: 21.90, 25.70, 29.30

1. Introduction

Recent studies of particle - γ coincidences using large γ -ray detector arrays in conjunction with 4π solid state particle-detector balls have shown that the particle trigger can be a decisive tool in identifying the final nucleus for a detailed nuclear spectroscopy [1, 2, 3, 4]. The enhanced emission of charged particles from the compound nucleus (CN) has also been discussed as a possible trigger for more strongly deformed shapes of the compound nucleus [5, 6, 7]. For lighter CN, in particular for $N=Z$ α -cluster nuclei, the emission of heavier fragments has been observed, and the process of the emission of ^8Be and ^{12}C nuclei is expected to be strongly enhanced if the CN is well deformed [8, 9, 10]. The emission of these “light” fragments (also called intermediate mass fragments) is actually viewed in close relation to asymmetric fission, which may proceed through strongly deformed shapes [11, 12].

We have started a study of the population of highly deformed bands in α -cluster nuclei by using binary reaction triggers [15, 16]. We have chosen reactions between light α -cluster nuclei populating CN in the $A=40$ -56 range, for which very deformed shapes are predicted [17]. In this paper we report results on the emission of ^8Be in the $^{32}\text{S} + ^{24}\text{Mg}$ reaction, which can be viewed as a binary process, at $E_L(^{32}\text{S}) = 130$ MeV, the ^{56}Ni CN being populated at an excitation energy of $E^* = 70$ MeV. The ^{56}Ni nucleus is of special interest in the sense that it can be populated by the mass-symmetric reaction $^{28}\text{Si} + ^{28}\text{Si}$, which is known to be one of the most favorable nuclear systems for the observation of resonant behavior [13]. Furthermore, the $^{28}\text{Si} + ^{28}\text{Si}$ scattering has revealed triaxial quasi-molecular states [12, 14] populated by the conjectured $J^\pi = 38^+$ resonance [13]. The symmetric and near-symmetric fission processes induced by the $^{32}\text{S} + ^{24}\text{Mg}$ reaction have been already studied extensively in the recent past [8, 9, 10, 11]. Previous γ -ray spectroscopy studies of this reaction, using the γ -spectrometer GASP (with an photopeak efficiency $P_{Ph} = 3\%$) with the light-charged-particle ball ISIS, have furnished detailed information on the structure of ^{48}Cr and other neighbouring nuclei, which were selected by gating on α -particles and protons [1, 3]. We have used the same original data [1] to search for γ -coincidences with ^8Be . The ^8Be nucleus is identified by selecting the corresponding events (as explained in Sect. 2) from the ΔE - E matrix shown in Fig. 1.

2. Experimental Procedures

The decay of ^8Be in its ground state, which is unbound by 0.0919 MeV, gives rise to 2 α -particles emitted in the laboratory system in a narrow cone of less than 5-7 degrees, which are registered simultaneously in one of the 40 ΔE - E telescopes of the ISIS multidetector array. The telescopes have an angular opening of $\Delta\theta \approx 29$ degrees, each with an insensitive gap of 6-7 degrees between two single detectors due to the width of the detector frames and cover 64% of 4π , whereas for the beam entrance and exit each one detector telescope has been taken out leading to an angular range from $\theta \simeq 16 - 164$ deg. The ^8Be events are thus easily registered as “pile up” events of 2 α -particles. The Li-isotopes could not be detected due to absorbers ($12\mu\text{m}$ Al foil) placed in front of the ISIS detectors, which modify also the ΔE - E curves of the detected particles. The detection efficiency for α -particles at the forward rings, which carries almost all of the statistics, is not affected by this absorbers.

The first excited state of ^8Be at an excitation energy of 3.04 MeV, having a width of 1.5 MeV, will produce an emission cone of more than 30 degrees. This means that only a small fraction of the 2α -pairs are registered in one ISIS telescope ($\approx 50\%$). A possibility to select such events is the selection of two α -particles in two adjacent telescopes, a procedure, which has also been pursued. These events show no difference in the γ -spectrum to the randomly distributed α -particle triggers, in contrast to those obtained with ^8Be -trigger as shown in Fig. 3. However, due to the high fraction of chance coincidences in the case of using two adjacent telescopes (see discussion below), it

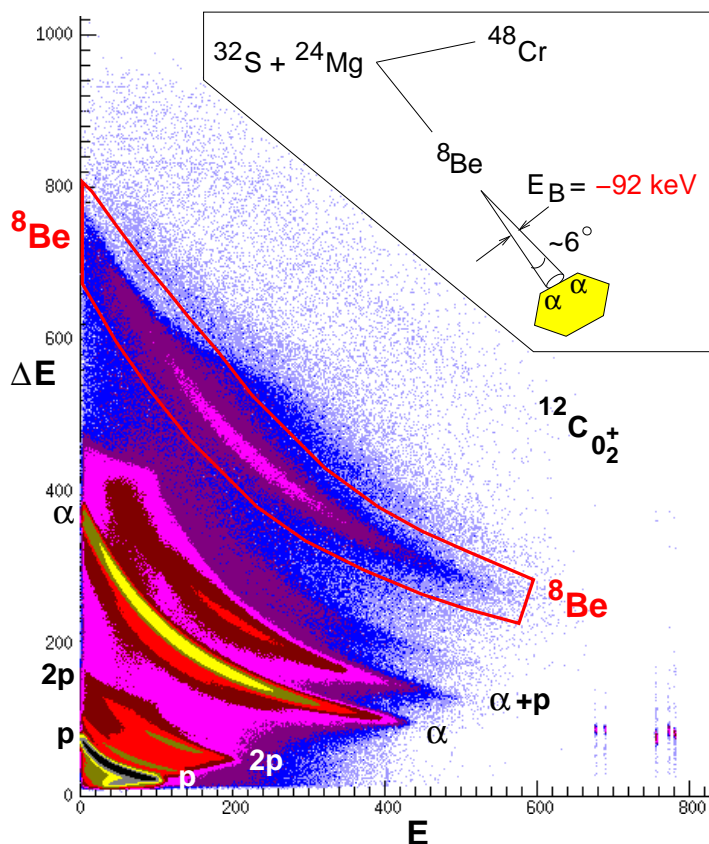


Figure 1. Plot of the ΔE - E signals from the ISIS telescopes as obtained from the experiment with $^{32}\text{S} + ^{24}\text{Mg}$ at $E_{\text{L}} = 130$ MeV. Events for the hydrogen isotopes p, d and t as well as for α -particles can be identified. The ^8Be events are seen at twice the amplitudes of the α -particles. The inset shows the breakup of $^8\text{Be}_{g,s}$ into 2 α -particles and their detection in the same detector (see text).

is necessary to ask e.g. for the sum of the kinetic energies of both registered α -particles in order to reduce the background of chance coincidences, but the two-dimensional ($E_{\alpha_1}/E_{\alpha_2}$) distribution shows no distinct structure for $^8\text{Be}_{0+}$ or $^8\text{Be}_{2+}$ states, and the energy resolution of the detectors (due to the large opening angle of the single telescopes, resulting in the coverage of a wide range of angles and α -energies) did not allow to make a selection of ^8Be states. Therefore these events of 2 α -particles in two adjacent detectors were not included in the data analysis. In the later analysis of the γ -spectra triggered with ^8Be a $^8\text{Be}_{2+}$ contribution can not be excluded, but it is not considered in the compound nucleus calculations in Sect. 4.

An important aspect of the identification of ^8Be is the determination of the background of chance coincidences resulting from 2 α -particles recorded in the same event in one of the N=40 ISIS telescopes in the ΔE - E branch for ^8Be . These 2 α -particles can either be emitted, (i) from the same event or, (ii) if emitted from two subsequent different events each emitting one α -particle, they must fall into the rise time of the electronics of the detection system of $\Delta t \approx 0.1 \mu\text{s}$ (“pile up” events).

The rate of chance coincidences of the latter type can be estimated by the expression $R_{2\alpha}^{ch} = R_\alpha \cdot R_\alpha \cdot \Delta t$, with R_α being the total rate for detection of single α -particle. From the total ISIS rates $R_\alpha = 488$ cps (counts/sec), $R_{2\alpha}^{ch} = 0.024$ cps and $R_{s_{Be}} = 9.95$ cps (integrated over all $N=40$ telescopes) we obtain the small average background value $R_{2\alpha}^{ch}/R_{s_{Be}} \simeq 0.24\%$, where $R_{s_{Be}}$ was not corrected for the background events included. For the most forward ISIS telescope ring, showing the highest counting rate (96% for the 2α case), the α and ^8Be rates and the background percentage can be given as a average value for a single detector by $R_\alpha = 77.9$ cps, $R_{s_{Be}} = 1.59$ cps and $R_{2\alpha}^{ch}/R_{s_{Be}} \simeq 0.04\%$, respectively.

The chance coincidence background due to two sequentially emitted α -particles from the same event hitting the same detector can be estimated from the multiplicity distribution, the solid angle Ω , and the efficiency ε of the individual telescopes. We choose the experimentally observed $\alpha - \alpha$ coincidences in two different telescopes as a reference point, which fixes the multiplicity of the events to $M_\alpha = 2$, with some very small contributions from higher multiplicities. The original average multiplicity is close to 1.05. As a first estimate we assume isotropic emission of both α -particles in the laboratory frame (thus neglecting e.g. kinematics). The total rate to observe a second α in coincidence with the first is given by the half of the total matrix of $N \cdot N$ combinations minus the diagonal part, which corresponds to the background in the true ^8Be events (N is the number of telescopes). This part of the matrix has $N(N - 1)/2 = 780$ elements; the corresponding total number of events measured in the experiment is $3.0 \cdot 10^6$ (2α) coincidences in 30.7 hours. The total background consisting of 40 diagonal elements (counters) in the matrix is determined by the ratio $40/780$ and must be scaled with the number of all observed $1.1 \cdot 10^6$ counts for ^8Be . We thus obtain a value of 14 % of 2α coincidences as background, a result, which is independent of the total efficiency to observe one α -particle. However, due to the kinematically inverted reaction, $^{32}\text{S} \rightarrow ^{24}\text{Mg}$, and due to the low energies in the center of mass system of the α -emitting nuclei, α -particle emission is strongly focused into the forward direction by kinematics. Another effect to be considered is the fact that for isotropic emission of the first α -particle in the c.m. system, the emission of the second α -particle is expected to be to some degree correlated in the plane of the emission of the first α -particle. This is reflected in the observation that 2α coincidences are stronger in telescopes with opposite directions to the beam for the most forward ISIS ring, enhanced by kinematical focusing towards $\theta_{c.m.} = 0^\circ$ and 180° . The enhanced counting rates at $\theta_{c.m.} = 0^\circ$ and 180° could not be analyzed quantitatively, because of the beam exit hole in the ISIS ball and due to the low energies of the backwards emitted α -particles in the laboratory system, which fall below the detection threshold. We observe 96% of the hits within the first ring of ISIS telescopes and 30% of the second α -particles are detected by ISIS telescopes on the opposite side in the ball within the same ring. From this fact the chance coincidence rate of 2 α -particles in one detector given above with 14% is estimated to be reduced by a factor of ≈ 2 . This factor results from the comparison of the theoretically estimated probability within the first ring of 6 detectors with a fixed detector for the first α , to

find the second α in the same detector, and the measured value for the probability to find the second α in the neighbouring detector. The latter should be very close to the probability to find it in the same detector (which is not directly measurable). The most intense $\alpha - \alpha$ coincidence rate for a given detector has been found not in the neighboring detector, but in the opposite side (reduction by typically a factor 2). The resulting value of 7% of the chance coincidence contribution of 2 α -particles in one detector is close to the measured value of finding the second α in other neighbouring detectors using the data of all adjacent detectors (i.e. also of the second ring), which is found to be 6%.

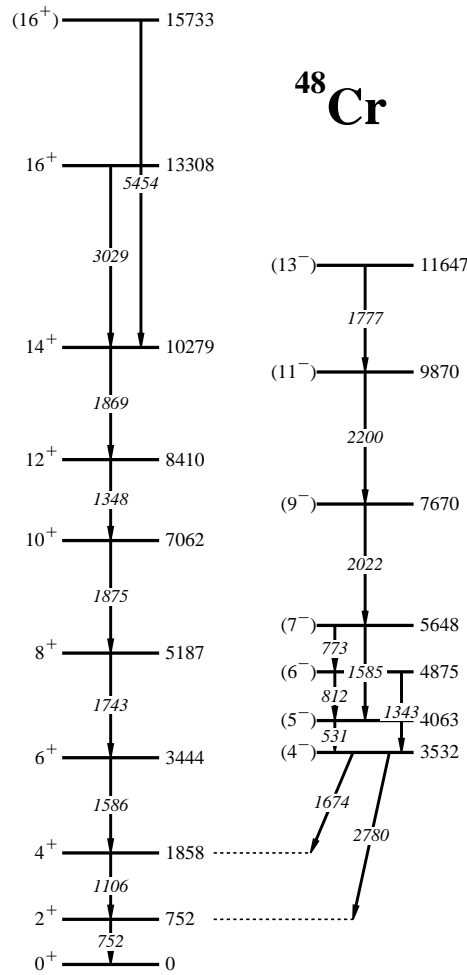


Figure 2. Decay scheme for ^{48}Cr as obtained from Ref. [21] with the γ -ray transitions used in the presentation of the relative yields in Fig. 5 and 6, where they are labeled by the decay energies shown in this figure. This level scheme shows only one excited side band.

In the following we will use the population of γ -ray decay bands in ^{48}Cr (the decay scheme is shown in Fig. 2) selected by coincidences with the multidetector array of Compton suppressed Ge γ -ray detectors, GASP, for a study of the properties of the binary decay channel, $^{56}\text{Ni} \rightarrow ^{48}\text{Cr} + ^8\text{Be}$. We note that also another binary channel can be selected with the prompt emission of 3 correlated α -particles from the second 0_2^+ in

^{12}C at $E^* = 7.654$ MeV, which decays by the emission of 3 α -particles (the γ -ray decay branch is $8.5 \cdot 10^{-3}$) with a total energy of 0.196 MeV. They are registered in one ΔE -E telescope as a triple pile up (see Fig. 1). γ -ray spectra of ^{44}Ti from this channel have been analyzed as well [16]. The triple chance coincidence rate for 3 α -particles in the ^{12}C ΔE -E branch is 0.26 % assuming an isotropic emission of the 3 α -particles.

The experimental details on the GASP and ISIS detector system can be found in the previous publications [1, 19, 20].

3. Experimental results for γ -ray yields connected to α -particle and ^8Be emission

The main aim of the present study is to test the selectivity of ^8Be emission as a trigger for γ -ray spectroscopy. As a first step we look into particle- γ -coincidence spectra for

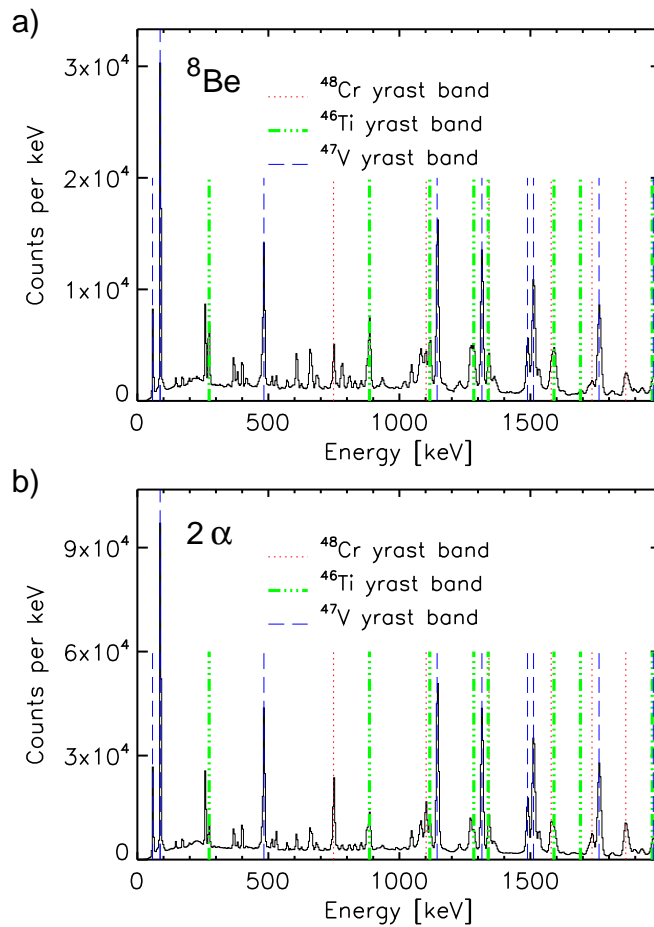


Figure 3. Particle-gated single γ -ray spectra. (a) Particle gate on ^8Be (b) Gate on 2 α -particles. The transitions within the ground state bands of ^{48}Cr , ^{47}V and ^{46}Ti are marked.

2 α -particles and ^8Be . They are shown in Fig. 3. The spectrum is dominated by the γ -

transitions of ^{47}V , the spectra are normalized to the same visual height of the 480 keV doublet line (478 keV and 484 keV) of ^{47}V . We observe very conspicuous differences between the two spectra: at first sight we recognise that the relative strength of the three residual nuclei is different: ^{48}Cr is reduced relative to ^{47}V in the case of ^8Be . Further ^{46}Ti is enhanced in the case of ^8Be , also relative to ^{47}V . The origin of these differences can be found in the difference in the excitation energy carried away by 2 α -particles as compared to ^8Be ; actually the compound decay calculations indicate that ^8Be leaves the residual nucleus (^{48}Cr) at higher excitation energy, thus partially explaining the enhanced emission of protons from $^{48}\text{Cr}^*$ towards ^{47}V and ^{46}Ti . In order to test the differences in the population in excitation energy and angular momentum it is useful to have a good knowledge of the decay scheme of the residual nuclei ^{48}Cr , ^{47}V and ^{46}Ti . In the further discussion we will use the known level scheme of ^{48}Cr [21] which is shown in Fig. 2. Similar analysis has been made for the cases of ^{47}V and ^{46}Ti [16], which are populated by the additional emission of one or two protons.

For a discussion of the individual decay schemes particle- γ - γ coincidences have to be projected. For a clear assignment of γ -ray transition energies such spectra are shown in Fig. 4, where we show the γ -decay spectra of ^{48}Cr . It should be mentioned that due to the long lifetime of the 4^- -state ($\tau \sim 4$ ns) *it is not possible to use γ -gated spectra to extract differences* in the population of the side band for different particle triggers, because within the lifetime the γ -emitting nucleus moves several centimeters and so the Doppler correction fails. For this reason all γ -yields given in the following discussion were extracted using the particle-gated single γ -ray spectra. Another reason to go back to the particle- γ matrices (projections of these are the spectra in Fig. 3) is that the statistics in γ - γ -yields would be reduced due to the efficiency of GASP by a factor of ≈ 33 . The integration of the γ -peaks can thus be done with smaller uncertainties. The analysis is done with the same procedure for both types of particle triggers. However, we have used the $\gamma - \gamma$ coincidences in order to detect cases with energy overlaps in the selection of the γ -transitions.

For the further analysis the decay scheme of ^{48}Cr (Fig. 2) is considered. The ground state band of ^{48}Cr is formed by the coupling of the 4 neutrons and 4 protons in the $f_{7/2}$ -shell, respectively, thus the main transitions observed in the spectrum (Fig. 4) are connected to the ground state band reaching up to spin $16\hbar$, the limit, which can be deduced from the 8 valence particles outside the $N=Z=20$ core. A backbend occurs at a spin value of $10\hbar$, the calculations of Caurier et al. [22] give the correct prediction of this behavior as well as a value for the quadrupole moment, which points to the cited deformation. The Nilsson diagram shown in Fig. 8 in Sect. 4, shows that the mixing with the $d_{3/2}^+$ shell is at the origin of the deformed shell and of the rotational character of the yrast levels of ^{48}Cr up to spin $16\hbar$. Inspecting the diagram of Fig. 8 we have also the possibility of obtaining a negative parity band by the excitation of one particle from the $[202]K = 3/2$ to the $[312]K = 5/2$ and possibly from the $[303]K = 7/2^-$ Nilsson orbit to the $[440]K = 1/2^+$ orbit of the $g_{9/2}$ shell for higher deformation. The $K = 4^-$ band is expected to have a larger deformation than the ground state band, because of the gain

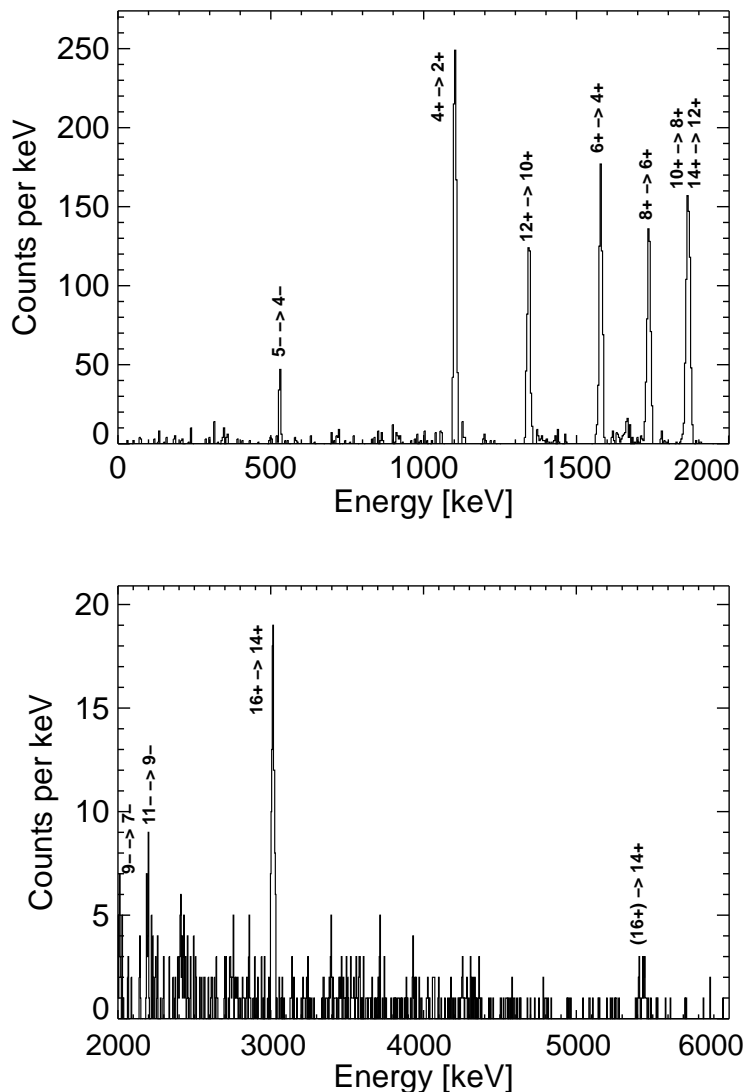


Figure 4. γ -ray spectra of ^{48}Cr obtained with a trigger on ^8Be in ΔE -E and a gate set on the $2^+ \rightarrow 0^+$ transition showing transitions in the ground state band and the $K = 4^-$ band.

in energy with increasing deformation. The first step in the analysis is the consideration of differences in the population of the higher spins in the ground state band of ^{48}Cr . For this purpose the γ -lines of the ground state band transitions were fitted in the particle-gated single γ -spectra. The fitting procedure in the high statistics spectra can be made identical so that differences observed should be due to differences in the feeding pattern. The comparison of the this obtained γ -yields for the particle trigger on ^8Be -particles relative to 2 α -particles, obtained by normalisation to the lowest transition ($2^+ \rightarrow 0^+$, 752 keV), is shown in Fig. 5. The normalization on the $2^+ \rightarrow 0^+$ transitions is a normalization to the g.s. band: the feeding of the 2^+ state from the 4^- -state ($\tau \sim 4$ ns)

of the side band (direct or via the 4^+ state) is suppressed, because the nucleus moves several centimeters during its lifetime, and therefore the Doppler correction causes an additional energy shift which is not taken into account in the determination of the peak area of the $2^+ \rightarrow 0^+$ transition, or these γ 's are not detected due to effective opening angle of the Ge's. In case of a thick target experiment, where the γ -emitting nucleus is stopped, the relative normalization as used in this work, would not be meaningful, because in that case the 2^+ state is fed by both bands and the effect of an enhancement of the population of the side band would not be seen.

Differences in the yields between the ^8Be - and the 2 α -particle triggers can be seen for the transitions at 1586 keV, 1875 keV, 1348 keV and 3029 keV. We observe an enhancement of 25% – 30% for the yields of the case with 1875 keV ($10^+ \rightarrow 8^+$, $14^+ \rightarrow 12^+$; this is a “double” line) and the case with 3028 keV ($16^+ \rightarrow 14^+$) transitions for the ^8Be -trigger. They are well separated and undisturbed, the result can be directly interpreted as due to an enhanced population of higher spins in the case of the emission of ^8Be from the compound nucleus.

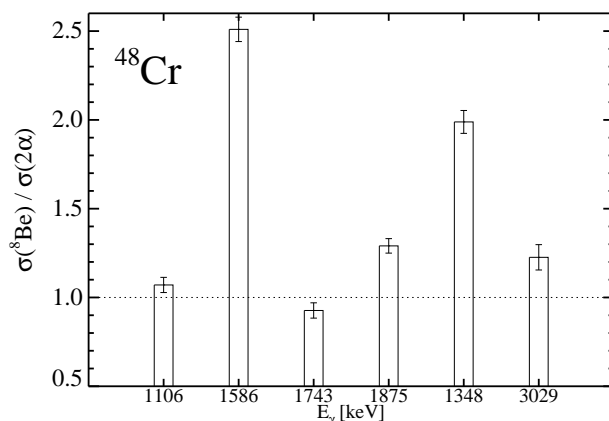


Figure 5. Comparison of experimental γ -ray yields in the gs-band of ^{48}Cr for triggers on ^8Be relative to those with 2 α -particles. The yields have been obtained by normalisation to the 752 keV transition (see Fig 2). γ -ray transitions are labeled by their energies. The error bars contain the statistical errors of the used γ -lines.

The enhanced γ -yields for the 1586 keV and 1348 keV transitions are influenced by overlapping γ -lines from another nucleus; the main contribution of this disturbance is due to unseparated γ -lines from ^{46}Ti at similar energies (1598 keV, 1345 keV), reflecting the stronger population of ^{46}Ti in the ^8Be case (see Fig. 3); only a small contribution is caused by the existence of side band transitions at this energies. The other relative γ -yields shown in Fig. 5 (1106 keV and 1743 keV) between low lying spins in ^{48}Cr differ only by less than 10% for the different particle triggers, i.e. no enhancement appears (as expected) for these cases.

In the second step of the analysis we considered the differences in the population of the side band for the different particle triggers. Fig. 6 shows yields of γ -lines of side

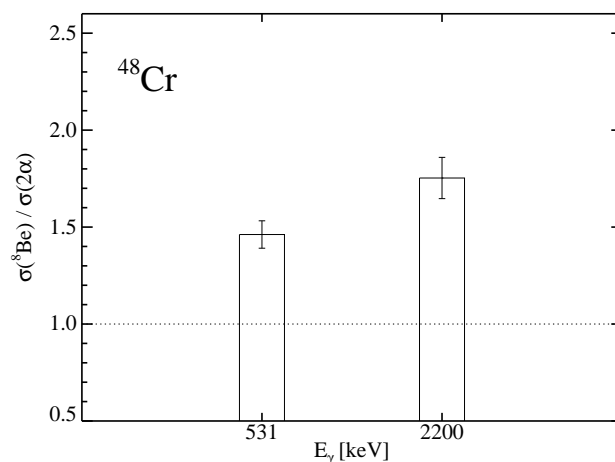


Figure 6. Experimental ratios of γ -ray yields in the side-band of ^{48}Cr (obtained as in Fig. 5) for triggers on ^8Be relative to those with 2 α -particles for γ -ray transitions in ^{48}Cr labeled by their energies (shown in Fig. 2).

band transitions for particle triggers on ^8Be relative to those with 2 α -particle, again each normalised to the $2^+ \rightarrow 0^+$ -transition (752 keV). For the side band the $5^- \rightarrow 4^-$ (531 keV) and the $11^- \rightarrow 9^-$ transition (2200 keV) were used which are free from contaminant lines. We see an enhancement by a factor of 1.5 and 1.8, respectively, for the particle trigger on ^8Be .

We will later relate this effect to a possible larger deformation of the side band. Similar observation of an enhanced population of a side band in a binary decay has been observed in a binary reaction $^{32}\text{S} + ^{24}\text{Mg}$ populating ^{28}Si ($K = 0_3^+$ -band) [10].

It should be mentioned that due to energy resolution and statistical reasons not all lines of the investigated bands could be used for the analysis. Further experiments with higher statistics are necessary to establish more cases.

We conclude that after the emission of ^8Be the population in excitation energy and angular momentum favors the $K^\pi = (4^-)$ side band of ^{48}Cr . The enhanced emission of ^8Be into deformed states of the daughter nucleus in statistical compound decay can be related to the differences in phase space in the emission process or to a structural preference for the emission of clusters as it is suggested by cluster model considerations [18]. As a first step we will consider the differences in 2α and ^8Be emission in the framework of the compound statistical decay using the extended Hauser-Feshbach method [23] described in the next section.

Similar analysis has been made for the neighbouring ^{47}V nucleus, which is reached from ^{48}Cr with high probability by a subsequent proton emission and also here an enhanced population of the deformed side band has been found in the binary case [16]. Since the decay scheme (c.f. [3]) is more complex than for ^{48}Cr and may not be complete, this case is not so well suited for the present discussion.

At the present stage the statistics is still too poor to examine the detailed population

patterns for the ^{44}Ti nucleus as populated by the 3α state of $^{12}\text{C}_{0_2^+}$ from the $^{44}\text{Ti}+^{12}\text{C}$ exit channel. Additional experiments are currently underway with GASP and EUROBALL to attack this problem.

4. Extended Hauser-Feshbach calculations for CN decay (fusion-evaporation and fusion-fission)

In the following the emission of ^8Be from a light CN is considered in the framework of the Extended Hauser-Feshbach Method (EHFM) as developed by Matsuse and collaborators [23]. In this approach the binary decay (i.e. fusion-evaporation of intermediate mass fragments and/or fusion-fission) of the CN is treated in addition to the well known process of fusion-evaporation of light particles (neutrons, protons, α). The method has been applied to several light-mass systems [23, 24, 25] in the compound nuclear masses region of $A=40-80$, and excellent agreement has been achieved with a standard set of parameters. For more details on the calculational procedures and a discussion of the sensitivity to the parameters of the model, we refer to Ref. [23]. However, for a better understanding of the dependence of the heavy fragment emission some parts of the formalism, which determine the decay probability, are also described hereafter. The partial width Γ_J for a decay channel with spin J is given by the relation

$$\Gamma_J = \frac{P_J}{2\pi\rho_J(\varepsilon)}, \quad (1)$$

where ρ_J is the level density as obtained by the usual Fermi gas expressions [26], ε the excitation energy in the daughter nucleus and P_J the phase space integral for the decay into the daughter nucleus. In the latter the transmission coefficients in the binary channel are of paramount importance, and thus indirectly the deformation of the two fragments, which will determine the Coulomb barrier. The total potential between the two fragments is parametrized as

$$V(L) = V_{\text{Coul}} + \frac{\hbar^2}{2\mu_f R_S^2} L(L+1) \quad (2)$$

Here the following definitions are used: μ_f – reduced mass in the center of mass (cm) system, R_S – the distance between the two fragments, which is defined as consisting of the two radii R_L and R_H and a neck-distance parameter d given by

$$R_S = R_L + R_H + d \quad (3)$$

From a recent systematic study [27, 28] of a large number of heavy-ion fusion-fission reactions (i.e. $^{28}\text{Si}+^{12}\text{C}$ [29, 30], $^{35}\text{Cl}+^{12}\text{C}$ [24], $^{36}\text{Ar}+^{12}\text{C}$ [31], $^{28}\text{Si}+^{28}\text{Si}$ [29], $^{32}\text{S}+^{24}\text{Mg}$ [9] and $^{35}\text{Cl}+^{24}\text{Mg}$ [25]) the given initial value of d used here to be $d = 3.0 \pm 0.5$ fm, has been found to have the following linear dependence with CN mass [28]: $d = 0.112(A_{CN} - 24.65)$. For R_L and R_H the radius parameter $r_0 = 1.2$ fm is commonly used ($R_{L,H} = r_0 A_{L,H}^{1/3}$) [23, 28]. In order to explain the present data consistently the adopted mass-dependence of the neck-distance parameter d , which is the only adjustable parameter of the EHFM scission point picture, is introduced to simulate the variation

of the CN deformation. It has been shown [11] that the shapes of the saddle- or scission-points, as assumed with the transition-state model and EHF_M, respectively, are almost identical. A longer neck, corresponding to a larger deformation, will give a reduced barrier height and thus a larger transmission probability. The deformation of the decaying system will thus enhance the emission of heavy fragments as already suggested by Blann [6].

The second effect, which will have a significant influence on the phase space integral is the level density $\rho_J(\varepsilon)$ in the daughter nucleus at spin J and excitation energy ε ,

$$\rho_J(\varepsilon) = \frac{1}{12} \left(\frac{a\hbar}{2\theta} \right)^{3/2} (2J+1)a \frac{e^{2\sqrt{X}}}{X^2} \quad (4)$$

$$X = a \left(\varepsilon - \frac{\hbar^2}{2\theta} J(J+1) - \Delta_{\text{pair}} \right) \quad (5)$$

The important parameters here are the level density parameter a and the moment of inertia θ , which determines the position of the yrast line of the daughter nucleus. For larger deformations the yrast line bends down, a larger phase space is obtained for the decay. In the initial version of EHF_M [23], the measured ground state binding energies are used to evaluate the excitation energy of the decaying fragment, but an average level density parameter was introduced. However, two sets of parametrizations are available for the level density parameter a used in each step of EHF_M. A constant value ($a = A/8$) was chosen for the preliminary calculations of Ref. [23]. This parameter set may overestimate shell effects. An alternative way to reproduce the strong variation from fragment to fragment is to incorporate shell effects in the level density formulas. In the present work (as well as in Refs. [24, 25, 27, 28]) shell corrections in the energy-dependent (temperature-dependent) level density parameter a are produced by the difference of the experimental mass and the liquid drop mass for each fragment. In order to introduce the shell effects in the level density parameter a , we use an improved version [28] of the empirical formula of Bohr and Mottelson [26]. The formula evaluates the shell structure energy which depends on the nuclear temperature T and consequently the level density parameter $a(T)$ becomes nuclear temperature dependent. To get the shell structure energy of the ground state, we use (see Refs. [25], for instance) the measured ground state binding energies and the liquid drop binding energies. This new modelization is currently being developed and will be discussed with the original EHF_M parametrization [23] in more detail in a forthcoming publication [28].

For the variations in the transmission coefficients in the binary channel we have varied the total distance R_S using the neck size parameter d , and the radius parameter r_0 . The results are illustrated in Fig. 7. We show actually the relative yield of ^8Be to 2 α -particles, both populating the same final ^{48}Cr nucleus. The dependence on other parameters of the EHF_M calculations are also shown: the primary L-value distribution determined by the maximum value of L , L_{cr} , and by its diffuseness Δ_J .

The experimentally determined ratios $\sigma(^8\text{Be})/\sigma(2\alpha)$ are shown by the horizontal lines in Fig. 7. The dashed line indicates the experimental value of the ratio for the whole

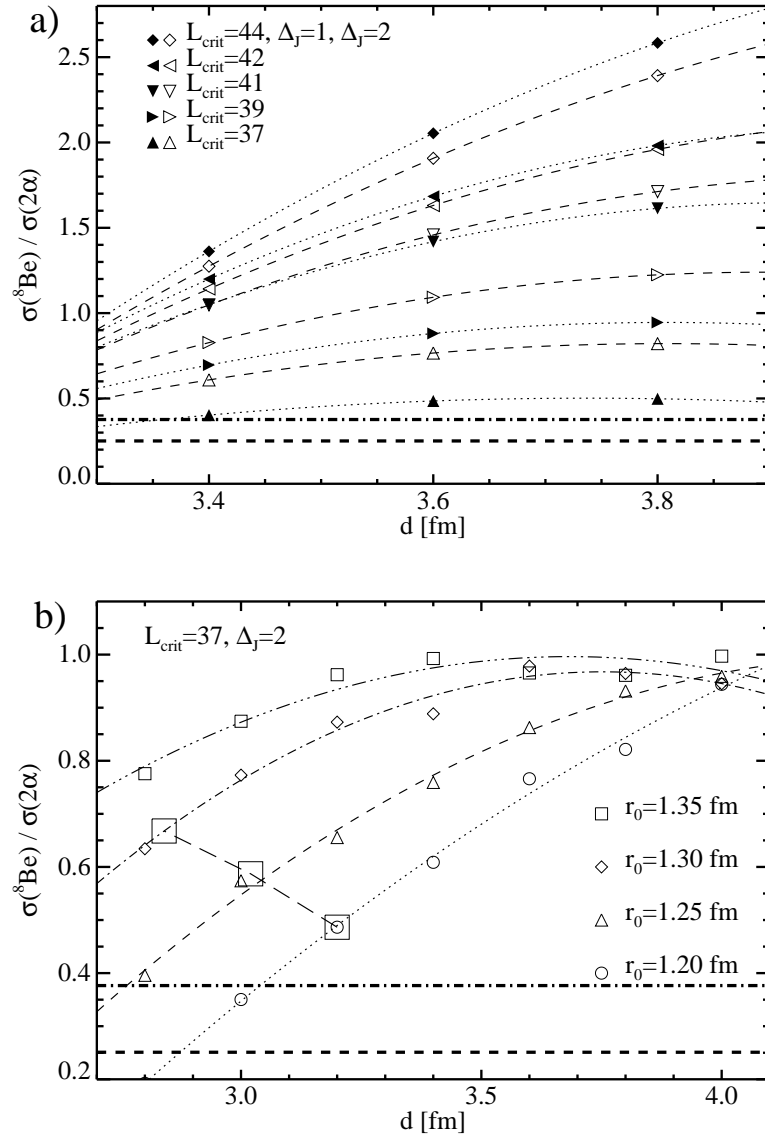


Figure 7. Ratio for the emission of ^8Be relative to two uncorrelated α -particles as obtained from the EHF M calculations as function of the deformation in a binary split, parametrized by the parameter d (neck size). a) Variation of L_{crit} and Δ_J . The filled symbols correspond to $\Delta_J = 1$, the open ones to $\Delta_J = 2$. The radius parameter r_0 was set to 1.2 fm. The experimental value of the ratio for the whole data set is indicated by the horizontal line. The second horizontal line is given by the enhancement factor determined from the γ -ray spectra as described before. b) Variation of r_0 for fixed values $L_{\text{crit}} = 37$ and $\Delta_J = 2$. The squares mark the r_0, d values for constant value of R_s (Eq. 3) but different moments of inertia.

data set, the dashed-dotted line is given by the enhancement factor determined from the γ -ray spectra as described before. It is difficult to compare this value directly with the calculated value, because the experiment does not cover the full 4π range (as described in Sect. 2), which is obtained in the calculation. In order to compare with the experiment we have to discuss the *relative changes* of the calculated ratio induced by the variation of the neck size parameter d , or by modifications in the angular momentum distribution in the incident channel. The result is shown in Fig. 7a. It can be observed that for the maximum spin values for the formation of the ^{56}Ni CN, $L_{cr} = 37 - 39\hbar$, adopted from Ref.[23] (consistent with the available measured complete fusion cross sections [32]), the ^8Be emission is not favoured relative to the 2α emission for more deformed states (at $d \approx 3.8$ fm). This result has also been observed in the work of Blann and Komoto [6]. Actually ^8Be carries more angular momentum and Fig. 7a shows that its emission will be favored at higher angular momenta ($L_{cr} > 40\hbar$) for larger deformations, as also predicted in Ref. [6]. It is interesting to note that the limiting angular momentum for ^{56}Ni is experimentally found to be close to $42\hbar$ [33] in agreement with the predictions of a modified version of the rotating liquid drop model (LDM), which includes finite-range corrections of the nuclear interaction by means of a Yukawa-plus-exponential attractive potential and diffuse-surface effects [34].

We consider in addition then a second effect, which is also discussed in Ref. [6], the increased phase space for the more strongly deformed daughter nuclei, i.e. for a softer yrast line due to a larger moment of inertia. In the present formulation this can be achieved by an increase of the radius parameter r_0 of the heavy fragment R_H . The result for different values of r_0 is shown in Fig. 7b, again as function of d , the neck parameter. The figure shows appreciable effects for changes of r_0 . We can read from this graphs also the effect produced by the larger moment of inertia alone by choosing $R_S(d, r_0) = \text{const.}$ Thus the constant values of R_S for ($d = 3.2$ fm, $r_0 = 1.20$ fm), for ($d = 3.02$ fm, $r_0 = 1.25$ fm) and for ($d = 2.84$ fm, $r_0 = 1.30$ fm) must be considered (they are marked as square symbols in Fig. 7b) and we deduce an enhancement of the $^8\text{Be}/2\alpha$ ratio by a factor ~ 1.7 for an increase of Θ by the factor $1.3/1.2 \sim 1.1$, which implies that for the present situation an increase of the moment of inertia of 10% of the daughter nucleus is reflected in a noticeable enhancement of the ^8Be yield by a factor 1.7. From these calculations we conclude that the changed ratio of the emission of ^8Be relative to that of two consecutive α -particles can be related to an increase of the deformation parameter β_2 of the heavier fragment, for which a discussion is given in the following section.

5. Decay scheme and deformed bands in ^{48}Cr

The structure of the ^{48}Cr nucleus is described quite well by the consideration of the half filled $f_{7/2}$ shell, which allows various nucleon excitations into higher orbitals.

The ground state band is suggested to have a deformation of $\beta_2 = 0.28$ [21] near the ground state and the deformation parameter reaches $\beta_2 = 0.1$, as the band termination

at $I = 16^+$ is approached. This decrease is explained by the fact that because of the relatively small number of nucleons in the $1f_{7/2}$ shell, it is not possible to obtain collectivity at high spins. In the case of the negative parity band, collectivity remains stronger also at higher spins due to the mixing with the $g_{9/2}$ shell. Even though the deformation at low spins is almost equal for the gs-band and the side band, the deformation at higher spins is larger for the side band. This is the crucial point when comparing the feeding into ^{48}Cr , because it occurs not nearby the ground state but at higher spins.

The result of the enhanced γ -ray yields for the ^8Be trigger for the side-band with negative parity ($K = 4^-$) can be related to higher deformations at high spins for this band. Particle-hole excitations from the $d_{3/2}$ to the $f_{7/2}$ orbit and also into the $g_{9/2}$ orbit of the next shell will be favored for larger deformations and higher spins. With these configurations a band head of $K = 4^-$ is obtained. Other side-bands with positive parity can be expected for the 2-particle–2-hole excitations to the $[310]1/2$ Nilsson orbital, which gives a band head with $K = 4^+$, but higher excitation energy than for $K = 4^-$. These features can be read qualitatively from the Nilsson diagram in Fig. 8.

6. Discussion and conclusions

The experimental observation of an enhanced emission of ^8Be into a more deformed side-band in ^{48}Cr has been observed by the use of particle - γ coincidences using a large γ -ray detector array. Using the *Extended-Hauser-Feshbach Method* (EHFM) it has been shown that cluster emission will be enhanced at high angular momenta for the decay into deformed residual nuclei. The result is related to previous theoretical and experimental studies of cluster emission from compound nuclei. In the work of Blann and Komoto [6] on cluster emission amplification, actually the case of the compound nucleus ^{56}Ni at an excitation energy of 94 MeV, somewhat higher than ours (70 MeV), has been treated. In their work deformation is introduced at various stages of the decay (mainly at the same places as in the present work), and the emission of clusters up to the mass ^{12}C is considered. They find that the fractional decay probability for α -particles varies only moderately with the introduction of deformation (at the maximum spin values of $40 - 45\hbar$); at these angular momenta an increase of the emission probability for ^8Be and ^{12}C by factors 2 – 4 is observed if the proper deformation values from LDM are introduced. The comparison of our result with Ref. [6] has to be seen with the constraint that in the previous work finite-range corrections, which produce for each angular momentum a lowering of the fission barrier due to the attractive forces between surfaces of the two nascent fragments at the saddle point [33], have not been taken into account. We can state that the present result and their work [6] are in agreement with the observation that the emission of heavier fragments at higher angular momenta is enhanced from and to deformed configurations. Our calculations have shown that this phenomenon depends on the maximum spin in the primary population, an effect which is also documented in [6].

The main origin of the enhancement in the population of more deformed shapes after the emission of ^8Be and ^{12}C might be linked to structural effects [35], like specific population of the states close to the yrast line. This feature will be pursued in a future investigation, where the population of large deformations of fragments from a binary process will be searched for in particle - γ coincidences with EUROBALL [15] and at higher incident energies.

Acknowledgments

This work has been started during a sabbatical leave of W. von Oertzen at the LNL. He would like to express his gratitude for the hospitality extended to him during this stay.

References

- [1] Lenzi S M *et al* 1996 *Z. Phys. A* **354** 117
- [2] Cameron J A *et al* 1996 *Phys. Lett. B* **387** 266
- [3] Cameron J A *et al* 1998 *Phys. Rev. C* **58** 808
- [4] Svensson C E *et al* 1998 *Phys. Rev. C* **58** R2621
- [5] Blann M 1980 *Phys. Rev. C* **21** 1770
- [6] Blann M and Komoto T T 1981 *Phys. Rev. C* **24** 426
- [7] Jaenker J *et al* 1999 *Eur. Phys. J. A* **4** 147, and references therein
- [8] Sanders S J *et al* 1988 *Phys. Rev. Lett.* **59** 2856
- [9] Sanders S J *et al* 1989 *Phys. Rev. C* **40** 2091
- [10] Sanders S J *et al* 1994 *Phys. Rev. C* **49** 1016
- [11] Sanders S J, Szanto de Toledo A and Beck C 1999 *Phys. Rep.* **311** 487, and references therein.
- [12] Nouicer R *et al* 1999 *Phys. Rev. C* **60** 041303
- [13] Betts R R, Back B B, and Glagola B G 1981 *Phys. Rev. Lett.* **47** 23
- [14] Beck C *et al* 2001 *Phys. Rev. C* **63** 014607
- [15] Gebauer B *et al* 1998 *EUROBALL proposal 98.31*
- [16] Thummerer S 1999 *Thesis, FU-Berlin*, and to be published.
- [17] Leander G and Larsson S E 1975 *Nucl. Phys. A* **239** 93
- [18] Zhang J, Merchant A C, and Rae W D M 1994 *Phys. Rev. C* **49** 562
- [19] Lenzi S M *et al* 1998 *Il Nuovo Cimento A* **111** 739
- [20] Farnea E *et al* 1997 *Nucl. Instrum. Methods A* **A00** 87
- [21] Brandolini F *et al* 1998 *Nucl. Phys. A* **642** 387
- [22] Caurier E 1995 *et al Phys. Rev. Lett.* **75** 2466
- [23] Matsuse T *et al* 1997 *Phys. Rev. C* **55** 1380
- [24] Beck C *et al* 1996 *Phys. Rev. C* **54** 227
- [25] Beck C *et al* 1998 *Eur. Phys. J. A* **2** 281
- [26] Bohr A and Mottelson B 1981 *Nuclear Structure*, Vol.II p.38, Benjamin Inc., 1981
- [27] Nouicer R 1997 *Thesis, Universite Louis Pasteur*, and 1997 *IReS Strasbourg, Report IReS* **97-34**
- [28] Beck C and Matsuse M to be published
- [29] Rousseau M 2001, *Thesis, Université Louis Pasteur, IReS Strasbourg Internal Report* 2001
- [30] Beck C *et al* 2000 *Ricerca Scientifica ed Educazione Permanente Supp.* 115, 407
- [31] Farrar K A *et al* 1996 *Phys. Rev. C* **54** 1249
- [32] Hinfefeld J D *et al* 1987 *Phys. Rev. C* **36** 989
- [33] Beck C and Szanto de Toledo A 1996 *Phys. Rev. C* **53** 1989
- [34] Sierk A J 1986 *Phys. Rev. C* **33** 2039
- [35] Freer M and Merchant A C 1990 *J.Phys. G* **23** 261 and refs. therein

